

DESMOSOME ASSEMBLY AND CELL-CELL ADHESION ARE MEMBRANE RAFT-DEPENDENT PROCESSES

Nataša Resnik¹, Kristina Sepčić², Ana Plemenitaš³, Reinhard Windoffer⁴, Rudolf Leube⁴, Peter Veranič¹

¹ University of Ljubljana, Faculty of Medicine, Institute of Cell Biology, Ljubljana, Slovenia

² University of Ljubljana, Biotechnical Faculty, Department of Biology, Ljubljana, Slovenia

³ University of Ljubljana, Faculty of Medicine, Institute of Biochemistry, Ljubljana, Slovenia

⁴ RWTH Aachen University, Institute of Molecular and Cellular Anatomy, Aachen, Germany

Address correspondence to: Peter Veranič, Institute of Cell Biology, Faculty of Medicine, University of Ljubljana, Lipičeva 2, SI-1000 Ljubljana, Slovenia, Tel:+386-1-543-7684, Fax:+386-1-543-7681, e-mail: peter.veranic@mf.uni-lj.si

The aim of our study was to investigate the association of desmosomal proteins with cholesterol-enriched membrane domains, commonly called membrane rafts, and the influence of cholesterol on desmosome assembly in epithelial MDCK cells (clone MDc-2). Biochemical analysis proved an association of desmosomal cadherin desmocollin 2 (Dsc2) in cholesterol-enriched fractions that contain membrane raft markers caveolin-1 and flotillin-1 and the novel raft marker ostreolysin. Cold detergent extraction of biotinylated plasma membranes revealed that ~ 60% of Dsc2 associates with membrane rafts while the remainder is present in non-raft and cholesterol-poor membranes. The results of immunofluorescence microscopy confirmed colocalization of Dsc2 and ostreolysin. Partial depletion of cholesterol with methyl- β -cyclodextrin disturbs desmosome assembly, as revealed by sequential recordings of live cells. Moreover, cholesterol depletion significantly reduces the strength of cell-cell junctions and partially releases Dsc2 from membrane rafts. Our data indicate that a pool of Dsc2 is associated with membrane rafts; particularly with the ostreolysin type of membrane raft and that intact membrane rafts are necessary for desmosome assembly. Taken together, these data suggest cholesterol as a potential regulator that promotes desmosome assembly.

Desmosomes are cell-cell junctions believed to resist mechanical stress in epithelia and cardiac muscle. A desmosome is made of two symmetrical halves, each composed of a transmembrane region and a plaque region that anchors intermediate filaments (IFs). Transcellular adherence between desmosomal cadherins, including desmocollins (Dscs) and desmogleins (Dsgs), depends on extracellular Ca^{2+} . In the cytosol, the tails of the desmosomal cadherins bind the cytosolic plaque proteins that mediate binding between cadherins

and IFs. In addition to the prominent biomechanical function, desmosomes have important roles in tissue morphogenesis and differentiation (1).

Cell membrane organization, with its structurally, compositionally and functionally distinct domains, contributes to the distribution of membrane proteins. Plasma membrane is composed of certain domains enriched with cholesterol and sphingomyelin, termed membrane rafts (MRs). The concept of MRs has evolved over the years; currently, they are defined as small (10-200 nm in diameter), heterogeneous and highly dynamic domains. However, these nanostructures can coalesce into larger, stable raft clusters (2). The majority of MRs are found in plasma membranes, while the remainder are present in exocytotic and endocytotic vesicles, in the Golgi apparatus and endoplasmic reticulum (3,4). MRs have been shown to accumulate proteins selectively, which in some cases directly interact with cholesterol and this interaction can affect the properties of the proteins (5,6). For example, MRs can dynamically organize specific membrane proteins (7) and promote the association and assembly of specific proteins. Consequently, membrane rafts facilitate signal transduction, protein import and trafficking (5,8). In relation to rafts, membrane proteins are assigned to three categories: those that are mainly found in rafts, those that are present in non-raft membranes, and those that represent an intermediate state, moving in and out of rafts (9).

On the basis of electron-microscopic observations, Lillemeier et al. (10) concluded that most or all plasma membrane-associated proteins are resident in cholesterol-enriched »islands«, which they further subdivided into raft and non-raft domains. However, in general, it is still believed that cell membranes are divided into high cholesterol raft domains and low cholesterol non-raft domains. The transmembrane proteins of cell-cell junctions, such as N-cadherins of adherens junctions (11,12) and occludin and specific claudins (4, 7) of tight junctions (13-15), have recently been

found in MRs, while E-cadherins of adherens junctions (16) and β 1 integrins (12,15) of focal contacts are excluded from these membrane domains. MRs contain various connexins but not complexes of gap junctions, showing that sometimes only individual junctional proteins cosediment with rafts (17).

The fact that there is a significant diversity in the composition of different raft preparations suggests that diversity among rafts exists. The most commonly used assay for the study of rafts is isolation of the buoyant detergent resistant membranes (DRMs) after extraction in cold Triton X-100. DRMs and, extrapolating, MRs can be identified by their marker proteins caveolin-1 (Cav), flotillin-1 (Flot) and a novel raft marker, ostreolysin (Oly). Oly is a protein from the oyster mushroom (*Pleurotus ostreatus*), which specifically recognizes the cholesterol/sphingomyelin-rich lipid phase, probably corresponding to the physical state of MRs (18,19). It should be kept in mind, however, that isolated DRMs do not fully represent biological rafts in size, structure and composition, since detergents can themselves induce the formation of ordered domains (20,21). To avoid those artifacts, a non-detergent sodium carbonate method or magnetic-bead immunoisolation approach should be used as an alternative for isolation of raft membrane fractions (22). Ultimately, a MR must be defined by its function, not by the method of isolation (23).

Despite the structural significance of MRs for individual desmosomal proteins desmoplakin (DP), plakoglobin (PG), Dsg2 as published elsewhere (24,25), it has not yet been confirmed whether Dsc2 and desmosomes as whole structures are associated to MRs. Additionally, the functional relationship between membrane rafts and desmosomes has not yet been clarified. The aims of this study were thus to examine the associations of desmosomal proteins with MRs and the role of cholesterol-enriched membrane domains for desmosome assembly and the strength of newly-formed (after 3 h of assembly) and well-established (after 1 day of assembly) cell-cell junctions. We determined that Dsc2, a broadly expressed desmosomal cadherin (26), is associated with MRs. Remarkably, other major desmosomal components, such as Dsg2, DP and cytokeratins (CKs), were also found in MRs, suggesting that complete desmosomes are raft-associated. The functional aspect of cholesterol participation in desmosomal structure was proven by its depletion with methyl- β -cyclodextrin (MCD), which prevented efficient desmosome assembly and weakened the strength of newly-formed and well-

established cell-cell junctions. On a biochemical level, MCD treatment resulted in partial release of Dsc2 from raft membranes, retaining distribution of Dsc2 in rafts when applying MCD loaded with cholesterol. The data suggest that assembly of desmosomes and the stability of cell-cell junctions are influenced by plasma membrane cholesterol.

EXPERIMENTAL PROCEDURES

Antibodies, fluorescent probes and reagents—The following antibodies against raft markers were used: anti-Cav, anti-Flot, anti-Oly (27) and Oly protein (27). Other antibodies used in this study were: anti-transferrin receptor, anti-GFP, anti-Dsc2, anti-DP, anti-Dsg2, anti-CK7 and anti-CK18 (mouse monoclonal; from Dako, Glostrup, Denmark). All the aforementioned antibodies were purchased from Abcam (Cambridge, UK) and were rabbit polyclonal unless stated otherwise. Alexa Flour 555-conjugated goat anti-rabbit was from Molecular Probes (Oregon, USA). Cy3-steptavidin was from Sigma-Aldrich (Steinheim, Germany). Methyl- β -cyclodextrin (MCD), cholesterol, cholesterol oxidase (CO) and EGTA were purchased from Sigma-Aldrich (Steinheim, Germany) unless stated otherwise.

Cell Culture—We used wild type MDCK cells and MDCK cells stably transfected with cDNA coding for Dsc2a-eYFP, designated MDc-2 cells (28). MDc-2 cells were maintained in a control medium composed of A-DMEM/F12 (1:1), 10% FCS, 50 U/ml crystacylin (Pliva, Zagreb, Croatia), 50 U/ml streptofatol (Fatol, Griefswald, Germany) at 37 °C, 5% CO₂. Cells were grown on plastic dishes (TPP, Trasadingen, Switzerland) and were subcultured with TrypLE Select at 90-100% confluence. Culture media and supplements were purchased from Invitrogen (Wien, Austria) unless stated otherwise.

Cholesterol depletion, repletion and EGTA treatment—To deplete membrane cholesterol from MDc-2 cells, we added sterile-filtered MCD medium (10 mM MCD solution made in a control medium with cholesterol free serum (HyClone, South Logan, Utah)) for the indicated period of time. MCD-cholesterol complexes were prepared as described by (29). Briefly, 6 mg of cholesterol was dissolved in 80 μ l of isopropyl alcohol:CHCl₃ (2:1). Two hundred mg of MCD was dissolved in 2.2 ml of water and heated to 80 °C. Cholesterol was added in small aliquots until the solution was clear. The MCD-cholesterol solution was filtered and added to cells with a final concentration of 10 mM. Cholesterol oxidase (1 U/ml) was added to a cholesterol-free medium for 2 h. EGTA solution (8

mM) was prepared in a control medium, sterile-filtered and applied to cells for 1 h.

Dispase-based dissociation assay—The assay was adapted from a previously described method (30). In brief, MDC-2 cells were seeded in triplicate on 30-mm plastic petri dishes. At ~70% confluence cells were treated with or without 10 mM MCD for 30 min, 1 h and 4 h or with MCD-cholesterol for 1 h. The cultures were then washed twice with warm (37 °C) PBS and incubated with 1.5 U/ml of dispase (Roche Diagnostic GmbH, Mannheim, Germany) for 15 min. The dispase solution was then carefully removed. Detached monolayers were dissolved in PBS and further subjected to 20 rounds of pipetting through a 200- μ l pipette. Cell dissociation was quantified by counting single cells per field of view (100 \times magnification, Leica DM IL). Experiments were performed three times in triplicate.

Cell surface biotinylation—MCD treated and untreated subconfluent MDC-2 cells were surface-labeled with cell impermeable EZ-Link Sulfo-NHS-SS-Biotin (Pierce Chemical, Rockford, USA) following the manufacturer's instructions. DRM isolation was then performed in cold Triton X-100 as described below. DRM fractions (6, 7) and non-DRM fractions (1-5 and 8-12) were collected in equal amounts and incubated with streptavidin beads. Biotinylated plasma membrane proteins were finally eluted by SDS-PAGE buffer and subsequently analyzed by Western blot as described below. In parallel, MDC-2 cells grown on coverslips were biotinylated as recommended and fixed with 4% formaldehyde (in PBS) for 15 min at 4 °C. Fixed cells were incubated with Cy3-conjugated streptavidin (1:100) for 30 min at 37 °C, and washed with PBS. Coverslips were mounted in Vectashield (Vector Laboratories, Burlingame, CA) and analyzed using an oil immersion objective (63 \times oil/NA 1.40) on a fluorescent microscope AxioImager Z1 (Carl Zeiss) supplemented with an ApoTome device.

Preparation of membrane fractions and cholesterol determination—

Detergent method ~70% confluent cells from 15-cm plastic petri dishes (~ 2.3×10^7 cells; TPP, Switzerland) were cultured in control media or were treated as indicated. After incubation, they were washed with cold PBS and collected by scraping and centrifugation at $200 \times g$ for 5 min. The pelleted cells were lysed for 30 min at 4 °C by 0.5% Triton X-100 in buffered saline (25 mM HEPES, 150 mM NaCl, 1 mM EDTA, 1 mM PMSF, and protease inhibitors (Roche Diagnostic GmbH, Mannheim, Germany), pH 6.5. Cell suspensions were passed 10 times through 22-gauge needles

during lysis and then mixed (1/1, v/v) with 85% sucrose (w/v) in buffered saline without Triton X-100. In a centrifuge tube, the resulting 42.5% sucrose mixture was overlaid successively with 35% and 5% (w/v) sucrose in buffered saline supplemented with 1 mM EDTA and 1 mM Na_3VO_4 . Following 18 h centrifugation at 4 °C (36,000 rpm, SW40 rotor, Beckman L8-M preparative centrifuge), 1-ml fractions were harvested from top to bottom; 400 μ l of each fraction was harvested for cholesterol measurements.

Detergent-free method— For detergent-free purification, we followed the method described by Song et al. (31). Briefly, cells were scraped into 500 mM carbonate buffer, pH 11 and homogenization and sonification were carried out sequentially. The homogenate was then adjusted to 45% sucrose by the addition of 90% sucrose prepared in MBS (25 mM Mes, pH 6.5, 0.15 M NaCl) and placed at the bottom of an ultracentrifuge tube. A 5–35% discontinuous sucrose gradient was formed above (5% sucrose/35% sucrose; both in MBS containing 250 mM sodium carbonate) and centrifuged at 36,000 rpms for 18h. Twelve 1-ml fractions were harvested from top to bottom of the gradient.

Lipids were extracted according to the method of Bligh and Dyer (32). Extracts were dried under a stream of N_2 and lipids redissolved in propanol. To determine the cholesterol concentration, we used Cholesterol Reagent (Thermo Fisher Scientific, Vantaa, Finland) according to the manufacturer's instructions.

Western-blot analysis—Aliquots of 50 μ l were taken from each 1-ml fraction of the sucrose gradients of treated and untreated cells, precipitated with TCA/acetone on ice, and resuspended in Tris-HCl (pH 8.7) and 2 \times Lamelli buffer at 37 °C. Samples were separated on either 10% or 12% SDS–polyacrylamide gels and then transferred to Hybond ECL nitrocellulose membranes (Amersham Biosciences, Buckinghamshire, UK), followed by incubation with the appropriate primary antibodies. Dsc2-YFP fusion proteins were detected with polyclonal anti-GFP antibodies, which are reactive against all variants of *Aequorea victoria* GFP, such as S65T-GFP, RS-GFP, YFP and EGFP. The bound primary antibodies were subsequently detected using HRP-conjugated secondary antibodies in conjunction with ECL detection reagents (Amersham Biosciences, Buckinghamshire, UK). Bands were visualized by exposure to and development of X-ray film. The grey values of band intensities were analyzed semi-quantitatively with Doc-ItLS image analysis software (UVP,

Cambridge, UK). A semi-quantitative amount of protein (arbitrary units) was defined as $N_x/(N_1+N_2+\dots+N_{12})\times 100\%$, where N_x is the intensity of an individual fraction band.

Ca²⁺-switch experiment and sequential recording of live cells—MDC-2 cells were cultured on glass bottom dishes with grid (MatTek Corporation, Ashland, MA, USA). After 1-h of EGTA treatment, EGTA was exchanged either with control or 10 mM MCD medium. Cells in culture dishes were immediately put on a microscope stage and locations on grid were selected. Three hours later, the cells were taken from the cell incubator and the desmosome assembly between cells at the same locations was examined with a fluorescent microscope AxioImager Z1 (Carl Zeiss) using 20× or 63× (water) objective.

Immunofluorescence—We examined colocalization of Dsc2-YFP with Cav, Flot or Oly in control cells and cells treated with 10 mM MCD for 1 h. Cells were grown on glass coverslips. Cells were washed with PBS, fixed in 4% paraformaldehyde (in PBS) for 10 min at 4 °C and permeabilized in 0.25% Triton X-100 for 10 min at 4 °C. After 30-min blocking with 2% BSA with 0.2% Na-azide (in PBS) at 37 °C, cells were incubated with anti-Cav (1:1000) or anti-Flot (1:500) primary antibodies for 1 h at 37 °C. Cells were washed with PBS and incubated with appropriate Alexa Fluor 555-conjugated secondary antibodies (1:1000) for 45 min at 37 °C. For labeling with Oly, the cells were incubated with 2.5 µg/ml Oly for 30 min at 37 °C, following by Oly anti-rabbit antibodies (1:2500) and then Alexa Fluor 555-conjugated secondary antibodies (1:1000). Coverslips were mounted in Vectashield (Vector Laboratories, Burlingame, CA) and analyzed using an oil immersion objective (63×oil/NA 1.40) on a fluorescent microscope AxioImager Z1 (Carl Zeiss) supplemented with an ApoTome device for optical sections generation. Images were acquired using the AxioVision programme.

RESULTS

Dsc2 is associated with membrane rafts (biochemical analyses)—The presence of Dsc2 in MRs was examined in isolated rafts, acquired after cold detergent extraction, which are operationally termed detergent resistant membranes (DRMs). As an alternative method, rafts were isolated by alkaline carbonate extraction. On the basis of protocols developed for MDCK cells (33), we isolated DRMs with cold 0.5% Triton X-100 from

light sucrose gradient fractions. Using this method, we tested whether Dsc2-YFP is associated with DRMs, identified by the raft markers Oly (Fig. 1A, fraction 6), Cav (Fig. 1A, fractions 6, 7), Flot (Fig. 1A, fractions 6, 7) or cholesterol enrichment (Fig. 1B, fractions 5, 6, 7). When those criteria were satisfied, we defined membrane fractions 6 and 7 as DRM fractions. Our isolated DRMs contained no TrfR, a marker of non-DRM regions (34), confirming the complete solubilization of non-raft membranes (Fig. 1A). Fractions 1-5 and 8-12, with a low cholesterol concentration (Fig. 1B, columns 1-4 and 8-12) and none or weak Oly, Cav or Flot band intensity (Fig. 1A, fractions 1-5 and 8-12), were defined as non-DRM fractions (fractions 1-5 and 8-12).

Protein profile analysis of the fractions from the sucrose gradient of whole cell membranes indicates that Dsc2-YFP is present in DRM fractions (Fig. 1C, fraction 6 and 7). A similar Dsc2 distribution in rafts was obtained in wild type MDCK cells (Fig. 1C), excluding the possibility that the presence of Dsc2 in rafts is due to protein overexpression. Additionally, it is known from previous work that Dsc2-YFP chimeras from MDC-2 cells are integrated into normal desmosomes and the fluorescence pattern is indistinguishable from that observed by immunofluorescence microscopy in wild type MDCK. Dsc2-YFP colocalizes with the desmosomal proteins plakoglobin, desmoplakin, desmoglein, plakophilin 2 and 3, indicating that transgene expression does not affect desmosome formation and composition (28). Dsg2, DP and CK7 and CK18 were also found in DRMs. The highest Dsc2 content, calculated from volume intensity measurements of 50-µl aliquots, was found in DRM fraction 6 (Fig. 1D). The possibility of raft fusion caused by detergent extraction, as well as lipid exchange between membranes led us to prepare membrane fractions with non-detergent isolation in a sodium carbonate buffer. Dsc2 abundant fractions contained Cav and Flot but not TrfR (Fig. 1E). This result verified Dsc2 association with MRs acquired with detergent isolation.

Dsc2 is associated with membrane rafts (light-microscopy analyses)—For colocalization of Dsc2 with raft markers, cells were immunostained for Oly, Cav and Flot. Cav and Flot were labeled with primary and secondary antibodies, whereas Oly was first applied to bind to rafts and further assessed with primary and secondary antibodies. The colocalization of Oly, Cav and Flot with Dsc2 was analyzed on optical sections. We observed that only Dsc2 and Oly colocalize significantly (Fig. 2A). No

clear colocalization between Dsc2 and Cav (Fig. 2B) and Dsc2 and Flot (Fig. 2C) was detected.

Plasma membrane Dsc2 associates with DRMs more than with non-DRMs—We restricted our further analysis to plasma membrane Dsc2, which actually contributes to desmosomal adhesion. To ascertain whether Dsc2 is associated with plasma membrane DRMs, we performed biotinylation of cell surfaces. Cell surfaces were labeled with impermeable EZ-Link Sulfo-NHS-SS-Biotin (Pierce) on ice to prevent biotinylation of intracellular membranes, enabling proper isolation of the plasma membrane. According to Cy3-streptavidin fluorescent labeling, Dsc2s were successfully biotinylated (Fig. 3A). Equal biotinylated aliquots were pooled from DRM and non-DRM fractions and analyzed with Western blot. Of the plasma membrane fraction, ~60 % of Dsc2 is related to DRMs and ~40% to non-DRMs ($p < 0.01$; Fig. 3B, C). Cav detection in biotinylated DRMs verified DRM purification. Comparably to our immunofluorescence studies, Flot was absent from plasma membrane DRM fractions and was present in unbiotinylated DRMs from endomembranes (Fig. 3B).

Biotinylation studies revealed two distinct pools of plasma membrane Dsc2: the bulk one associated with DRM domains and related to high cholesterol levels and the second associated with non-DRM.

Membrane rafts are necessary for effective desmosome assembly and stabilization of newly-formed cell-cell junctions—The aforementioned results led us to examine whether MR disruption caused by cholesterol sequestration have any impact on desmosome assembly. The Ca^{2+} -chelating agent EGTA provoked separation of desmosome halves, a process that was followed by cell rounding and Dsc2 internalization, which has been described elsewhere (35), (Fig. 4A, A', C, C'). Cells were then left for 3 h to assemble desmosomes in control or MCD medium. Culturing in control medium led to a confluent state in which cells revealed the original polygonal cell shape with well-established desmosomes (Fig. 4D, D', D''). Cells in MCD medium did not reach cell confluence to the same extent as in the control medium, intercellular spaces frequently remained (Fig. 4B', B'', asterisk, arrowhead) and desmosomes were not assembled on entire cell surfaces (Fig. 4B, B', B''). Additionally, MCD prevented a polygonal cell shape. The stability of cell junctions in the MCD medium was decreased because the strength of cell-cell junctions was weaker when assembled in MCD medium. The strength of newly-formed cell-cell junctions was presented with reference to

well-established cell-cell junctions built after 24 h of culturing (control cells). The ratios between dissociated cells after 3 h of assembly in MCD and the control medium in relation to well-established cell-cell junctions built after 24 h of culturing were 3.9 and 2.8 ($p < 0.05$), respectively. These data indicate that MRs are necessary for normal desmosome assembly and stabilization of newly-formed cell junctions.

Depletion of plasma membrane cholesterol reduces the strength of well-established cell-cell junctions—We investigated how cholesterol sequestration affects the strength of well-established cell-cell junctions (established after 1 day of culturing). For desmosome-mediated adhesion in MDCK cells, it is known that desmosomal adhesion progressively develops over a period of time, reaching a plateau at 24-32 h (36). In our study, the cells were cultured for 30 min, 1 h and 4 h in 10 mM MCD. Using a dispase-based dissociation assay, the ratios between dissociated cells treated for 30 min in MCD and cells in control was 1.2 (± 0.057) and increased to 2.3 (± 0.258) when cells were treated with MCD for 1 h. Four-hour incubation in MCD raised the ratio to 3.9 (± 0.343) (Fig. 5). The strength of cell-cell junctions was retained, in comparison to the control, when complexes of MCD-cholesterol were added (1 ± 0.356). With 30-min (Fig. 5A) and 1-h incubation (Fig. 5B) in MCD, the Dsc2 distribution remained continuous. After 4-h incubation in MCD, free extracellular spaces at the cell edges appeared, resulting in discontinuous Dsc2 distribution, although desmosomes were still maintained (Fig. 5C). Cell viability tested with trypan blue staining after 4h incubation in MCD had not declined (data not shown). After MCD treatment (1 h in 10 mM MCD), Oly labeling was dramatically decreased, showing successful disruption of the rafts (Fig. 6A, MCD treatment). MCD treatment revealed a partial release of Dsc2 from DRM and non-DRM fractions. The release was significant for DRM fractions 6 and 7 in comparison to the control (Fig. 6B) although some Dsc2 still persisted in DRM fraction 7 (Fig. 6B) after MCD treatment. Similarly, Dsg2 was released from DRMs (Fig. 6C). After applying MCD-cholesterol, Dsc2 distribution prevailed in DRMs (Fig. 6B, fraction 6 and 7). Complete Dsc2 escape from DRM fractions was achieved with cholesterol oxidase (CO), which oxidizes cholesterol to cholestenone (Fig. 6B). These data indicate that cholesterol also contributes to the strength of well-established cell contacts and to Dsc2 partitioning in DRMs.

DISCUSSION

The results of the presented study led us to the conclusion that desmosome assembly and the strength of cell-cell junctions depend on cholesterol-enriched domains, also designated membrane rafts. An earlier work concerning the lipid composition of the desmosomal area of the plasma membrane revealed that the desmosomal enriched fraction from cow nose epidermis consists of 10% lipids, of which the cholesterol fraction is estimated at 40% (37). This value revealed desmosome preference for a cholesterol environment. On the basis of these data, we first sought to determine the association of desmosomes with MRs and how MRs contribute to desmosome assembly. The structural significance of MRs for individual desmosomal proteins DP, PG, Dsg2 has been published elsewhere (24,25), but it has not yet been confirmed that Dsc2 and desmosomes are associated to MRs as whole structures. Our main approach was to use detergent isolation of MRs, operationally termed DRMs. It is known that after detergent extraction only a few proteins retain associations with lipids and are recovered in DRMs, indicating a strong interaction (33). On the other hand, theoretical and experimental findings provide evidence against identifying DRMs with rafts; hence non-detergent purification of membrane domains was used to confirm results given by detergent isolation. Both methods revealed that Dsc2 is present in membrane domains with typical characteristics of membrane rafts. Furthermore, we restricted our initial analysis of Dsc2 from whole cell lysates to plasma membrane in order to avoid mixing Dsc2s from different subcellular sources. Two distinct pools of Dsc2 existed in the plasma membrane: the bulk one associated with DRMs, which is related to high cholesterol concentrations and the second one associated with non-DRMs. This is in agreement with the results of Kahya and coworkers (38), which showed that only a fraction of the membrane proteins are associated with rafts and these proteins usually partition between raft and non-raft regions. Additionally, in raft fractions, we found representative proteins for all the main structural parts of a desmosome: the transmembrane proteins Dsg2, the plaque protein DP, and cytoskeletal elements CK7 and CK18. Since all essential components of desmosomes reside within rafts and it has been confirmed that fusion Dsc2-YFP proteins are highly enriched in typical desmosomes (28), we assume that whole desmosomal structures are present in rafts.

As mentioned before, the presence of proteins in DRMs obtained with Triton X-100 does not necessarily indicate association with the same domains in the native membranes. The association of plasma membrane Dsc2 with natural rafts was therefore demonstrated by immunofluorescence. We used raft markers Cav, Flot and Oly to confirm the Dsc2 association with membrane rafts. The immunocolocalization of Dsc2-Oly was very evident but not in the case of Dsc2-Flot and Dsc2-Cav. On the basis of these results, we propose that multiple types of rafts exist, with heterogeneous protein composition (23). We used a novel raft marker Oly, which selectively binds to membrane domains with specific a cholesterol: sphingomyelin ratio. Our biochemical and immunolabeling results thus confirm the raftophilic nature of desmosomes.

Cholesterol was found to promote the assembly and to stabilize the adherens junctions of non-epithelial cells (11), which are structurally and functionally very similar to desmosomes. In spite of the evidence that cholesterol is needed to maintain the organization and, therefore, the integrity of non-epithelial adherens junctions and tight junctions (12,14), interactions at the molecular level between cholesterol and junctional proteins are still unknown. Our choice of MCD as the cholesterol depleting agent was primarily based on the fast and selective depletion of cholesterol from the plasma membrane (39). Moreover, the efficiency of depletion of cholesterol from raft regions appears to be higher than from non-raft regions (40). Secondly, short-term use of MCD does not affect the metabolic activity of cholesterol synthesis. Our results verified that, after 1-h incubation in 10 mM MCD (the amount of cholesterol is reduced by ~30%), the membrane domains with an affinity to raft marker Oly completely disappeared, as deduced from the almost complete absence of an immunofluorescent signal for Oly. Desmosome assembly in MCD-treated cells occurred, however at a clearly lower extent in comparison to the assembly in control medium. After 3 h of incubation in MCD, the strength of the cell-cell junctions was decreased, probably due to the reduced number of functional desmosomes. Additionally, the change in cholesterol concentration might modify the physical environment of the remaining raft and affect the content of membrane domains (23), resulting in improper lipid to protein interactions required for desmosome assembly. We found that MCD treatment also severely disturbs the stability of well-established cell-cell junctions, implying a major influence of cholesterol on the basic adhesive

function of desmosomes. Four-hour treatment in MCD dramatically decreased the strength of cell-cell junctions. Similar to tight junction maintenance in MCD medium (41), desmosomes were still preserved on the plasma membrane even after 4-h treatment in MCD. Decreases in the strength of cell-cell junctions may be a consequence of reduced interaction between the desmosomal proteins. As found for LFA-1, the leukocyte membrane raft protein, the cholesterol concentration must exceed a critical threshold for the proper function of LFA-1 (42). Lipid enclosure may also contribute to the functionality of desmosomal proteins and assure the maximum strength of desmosomal adhesion. In MCD-treated cells, Dsc2 was released from DRMs, while treatment of cells with MCD-cholesterol retained Dsc2 in DRMs, proving a cholesterol specific sequestration with MCD and the importance of cholesterol for the interaction with Dsc2. In MCD-treated cells, some Dsc2 still persisted in DRMs and its distribution on the cell surface remained almost unchanged. This implied that desmosomes are not functional, although they are maintained. Cells might also be able to maintain DRMs in cholesterol-depleted medium by redistributing the remaining cholesterol. In our study, a complete displacement of Dsc2 out of rafts was achieved with cholesterol oxidase, suggesting that severe raft disruption is needed to impair desmosome-associated rafts.

In conclusion, our results indicate that desmosomes are membrane raft-associated structures, the assembly and distribution of which depends on membrane rafts. Membrane rafts may therefore be involved in desmosome regulation.

REFERENCES

1. Garrod, D. R., Merritt, A. J., and Nie, Z. (2002) *Curr. Opin. Cell Biol.* **14**, 537-545
2. Kusumi, A., Koyama-Honda, I., and Suzuki, K. (2004) *Traffic* **5**, 213-230
3. Ikonen, E. (2001) *Curr. Opin. Cell Biol.* **13**, 470-477
4. Browman, D. T., Resek, M. E., Zajchowski, L. D., and Robbins, S. M. (2006) *J. Cell Sci.* **119**, 3149-3160
5. Simons, K., and Toomre, D. (2000) *Nat. Rev. Mol. Cell Biol.* **1**, 31-39
6. Epand, R. M. (2006) *Prog. Lipid Res.* **45**, 279-294
7. Mineo, C., James, G. L., Smart, E. J., and Anderson, R. G. (1996) *J Biol Chem* **271**, 11930-11935
8. Pike, L. J. (2003) *J. Lipid Res.* **44**, 655-667
9. Simons, K., and Eehalt, R. (2002) *J. Clin. Invest.* **110**, 597-603
10. Lillemeier, B. F., Pfeiffer, J. R., Surviladze, Z., Wilson, B. S., and Davis, M. M. (2006) *Proc. Natl. Acad. Sci. U. S. A.* **103**, 18992-18997
11. Causeret, M., Taulet, N., Comunale, F., Favard, C., and Gauthier-Rouviere, C. (2005) *Mol. Biol. Cell* **16**, 2168-2180
12. Nakai, Y., and Kamiguchi, H. (2002) *J. Cell Biol.* **159**, 1097-1108
13. Lambert, D., O'Neill, C. A., and Padfield, P. J. (2005) *Biochem. J.* **387**, 553-560
14. Lambert, D., O'Neill, C. A., and Padfield, P. J. (2007) *Cell. Physiol. Biochem.* **20**, 495-506
15. Nusrat, A., Parkos, C. A., Verkade, P., Foley, C. S., Liang, T. W., Innis-Whitehouse, W., Eastburn, K. K., and Madara, J. L. (2000) *J. Cell Sci.* **113**, 1771-1781
16. Baumgartner, W., Wendeler, M. W., Weth, A., Koob, R., Drenckhahn, D., and Gessner, R. (2008) *J. Mol. Biol.* **378**, 44-54
17. Locke, D., Liu, J., and Harris, A. L. (2005) *Biochemistry* **44**, 13027-13042
18. Sepcic, K., Berne, S., Rebolj, K., Batista, U., Plemenitas, A., Sentjurc, M., and Macek, P. (2004) *FEBS Lett.* **575**, 81-85
19. Chowdhury, H. H., Rebolj, K., Kreft, M., Zorec, R., Macek, P., and Sepcic, K. (2008) *Toxicol* **51**, 1345-1356
20. Heerklotz, H. (2002) *Biophys. J.* **83**, 2693-2701
21. Lichtenberg, D., Goni, F. M., and Heerklotz, H. (2005) *Trends Biochem. Sci.* **30**, 430-436
22. Shah, M. B., and Sehgal, P. B. (2007) *Methods Mol. Biol.* **398**, 21-28
23. Pike, L. J. (2004) *Biochem. J.* **378**, 281-292
24. Nava, P., Laukoetter, M. G., Hopkins, A. M., Laur, O., Gerner-Smidt, K., Green, K. J., Parkos, C. A., and Nusrat, A. (2007) *Mol. Biol. Cell* **18**, 4565-4578
25. Morel, E., Fouquet, S., Chateau, D., Yvernault, L., Frobert, Y., Pincon-Raymond, M., Chambaz, J., Pillot, T., and Rousset, M. (2004) *J. Biol. Chem.* **279**, 1499-1505
26. Nuber, U. A., Schafer, S., Schmidt, A., Koch, P. J., and Franke, W. W. (1995) *Eur. J. Cell Biol.* **66**, 69-74
27. Berne, S., Krizaj, I., Pohleven, F., Turk, T., Macek, P., and Sepcic, K. (2002) *Biochim. Biophys. Acta* **1570**, 153-159
28. Windoffer, R., Borchert-Stuhltrager, M., and Leube, R. E. (2002) *J. Cell Sci.* **115**, 1717-1732
29. Pike, L. J., and Miller, J. M. (1998) *J. Biol. Chem.* **273**, 22298-22304
30. Huen, A. C., Park, J. K., Godsel, L. M., Chen, X., Bannon, L. J., Amargo, E. V., Hudson, T. Y., Mongiu, A. K., Leigh, I. M., Kelsell, D. P., Gumbiner, B. M., and Green, K. J. (2002) *J. Cell Biol.* **159**, 1005-1017
31. Song, K. S., Li, S., Okamoto, T., Quilliam, L. A., Sargiacomo, M., and Lisanti, M. P. (1996) *J. Biol. Chem.* **271**, 9690-9697
32. Bligh, E. G., and Dyer, W. J. (1959) *Can. J. Biochem. Physiol.* **37**, 911-917
33. Schuck, S., Honsho, M., Ekroos, K., Shevchenko, A., and Simons, K. (2003) *Proc. Natl. Acad. Sci. U. S. A.* **100**, 5795-5800
34. Smart, E. J., Ying, Y. S., Mineo, C., and Anderson, R. G. (1995) *Proc. Natl. Acad. Sci. U. S. A.* **92**, 10104-10108
35. Matthey, D. L., and Garrod, D. R. (1986) *J. Cell Sci.* **85**, 113-124
36. Matthey, D. L., Burdge, G., and Garrod, D. R. (1990) *J. Cell Sci* **97 (Pt 4)**, 689-704

37. Skerrow, C. J., and Matoltsy, A. G. (1974) *J. Cell Biol.* **63**, 524-530
38. Kahya, N., Brown, D. A., and Schwillie, P. (2005) *Biochemistry* **44**, 7479-7489
39. Kilsdonk, E. P., Yancey, P. G., Stoudt, G. W., Bangerter, F. W., Johnson, W. J., Phillips, M. C., and Rothblat, G. H. (1995) *J. Biol. Chem.* **270**, 17250-17256
40. Zidovetzki, R., and Levitan, I. (2007) *Biochim. Biophys. Acta* **1768**, 1311-1324
41. Suzuki, T., Matsuzaki, T., Hagiwara, H., Aoki, T., Tajika-Takahashi, Y., and Takata, K. (2006) *Act. Histochem. Cytochem.* **39**, 155-161
42. Marwali, M. R., Rey-Ladino, J., Dreolini, L., Shaw, D., and Takei, F. (2003) *Blood* **102**, 215-222

FOOTNOTES

The authors thank Mr Martin Cregeen for checking the English of the text.

The abbreviations used are: A-DMEM, Advance-Dulbecco's modification of Eagle's medium; A.U., arbitrary units; BSA, bovine serum albumin; Cav, caveolin; CK7, cytokeratin 7; CK20, cytokeratin 20; CO, cholesterol oxidase; Cy3, cyanine 3; Dsc2, desmocollin 2; DP, desmoplakin, Dsg2, desmoglein 2; DRM, detergent resistant membrane; FCS, fetal cow serum; Flot, flotillin; GFP, green fluorescent protein; HEPES, 2-[4-(2-hydroxyethyl)piperazin-1-yl]ethanesulfonic acid; HRP, horseradish peroxidase; IFs, intermediate filaments; Mes, 2-(*N*-morpholino)ethanesulfonic acid; MCD, methyl- β -cyclodextrin; MR, membrane raft; non-DRM, non-detergent resistant membrane; Oly, ostreolysin; PBS, phosphate buffer saline; TrfR, transferrin receptor; eYFP, enhanced yellow fluorescent protein.

FIGURE LEGENDS

Fig. 1. Dsc2 associates to DRMs of MDc-2 cells. A, DRMs were pooled from sucrose gradients after centrifugation of Triton X-100 lysed cells; 50 μ l of each fraction (1-12) was added on SDS-PAGE gels and proteins were detected by Western blot. The distribution of ostreolysin (Oly), caveolin (Cav), flotillin (Flot), transferrin receptor (TrfR) in each fraction. Fractions positive for raft markers (Oly, Cav, Flot) and rich in cholesterol content were determined as DRMs (fractions 6, 7). B, the profile of the cholesterol concentration in fractions from top to bottom (1-12) of the sucrose gradient acquired from cells extracted with Triton X-100. DRM fractions 6, 7 exhibit a cholesterol peak. C, DRMs contained desmosomal proteins Dsc2-YFP, Dsc2 in wild type MDCK, desmoglein 2 (Dsg2), desmoplakin (DP), cytokeratin 18 and 7 (CK18 and CK7). D, the graph demonstrates the volume intensity profile in arbitrary units (A.U.) of Dsc2 in 50- μ l of control fractions. Fraction 6 from DRMs shows the highest intensity. Representative blots from three separate experiments are shown. Error bars represent the SEM from an experiment in which each condition was tested in triplicate. E, Dsc2 associates to rafts acquired with detergent-free isolation. Membrane fractions were prepared using the carbonate step gradient method (non-detergent); 50 μ l of each fraction (1-12) was added on SDS-PAGE gels and proteins were detected by Western blot. Distributions of Cav, Flot, TrfR and Dsc2 in carbonate-based fractions. Fractions 5, 6, 7, 8 were determined as raft fractions due to their Cav and Flot inclusion and TrfR exclusion.

Fig. 2. Dsc2 colocalizes with MRs. Representative optical sections of MDc-2 cells, double-labeled with Dsc2-YFP and antibodies against ostreolysin (Oly), caveolin (Cav) or flotillin (Flot). Right hand panels show colocalization in merged images of Oly and Dsc2 (A), Cav and Dsc2 (B), or Flot and Dsc2 (C). Cells were stained as described in Materials and Method. Scale bar: 10 μ m.

Fig. 3. Dsc2 associates with DRMs in the plasma membrane. A, immunofluorescent labeling shows that Dsc2-YFP (left panel) was successfully biotinylated (Cy3-streptavidin), as evident from the merged image. Scale bar, 10 μ m. B, biotinylated DRMs (column 1) and non-DRMs (column 2) from MDc-2 cells were collected and analyzed with Western blot. Distribution of Dsc2-YFP in biotinylated DRMs and non-DRMs. Distribution of Cav and Flot confirms that DRMs are not contaminated with non-DRMs. Similarly, Flot distribution in non-biotinylated fractions confirms that DRM fractions

originate from the cell surface. Representative blots from three separate experiments are shown. C, the distribution of Dsc2-YFP in biotinylated DRMs and non-DRMs shows the greatest intensity in the DRM biotinylated fraction ($p < 0.01$). Error bars represent the SEM from an experiment in which each condition was tested in triplicate.

Fig. 4. Desmosome assembly in MCD medium is restricted. After 1 h of EGTA treatment cells became rounded and had internalized Dsc2-YFP (A and corresponding fluorescent image A'; C and corresponding fluorescent image C'). EGTA was then replaced with MCD (B) or control (D) medium and cells were left to attach for 3 h. Desmosome assembly in MCD medium was incomplete, intracellular spaces were left (B', B'', asterisk, arrowhead) and a polygonal shape was not achieved (B). In the control medium, desmosomes become assembled, the cells achieved a polygonal shape (D' and D'') and established confluent islands (D). Dashed squares represent locations from which high magnifications were taken. E, the strength of newly-formed cell-cell junctions was found to be weaker than in the control medium after 3 h of assembly. The ratios between dissociated cells after 3 h of assembly in MCD and control medium with regard to well-established cell junctions built after 24 h of culturing were 3.9 and 2.8 ($p < 0.05$), respectively. Error bars represent the SEM from an experiment in which each condition was tested in triplicate.

Fig. 5. Depletion of cholesterol reduces the strength of well-established cell-cell junctions. Disperse-based dissociation assay revealed that a diminished concentration of membrane cholesterol loosened cell-cell junctions and, consequently, reduced the number of cell-cell junctions. Each column represents the ratio between the number of dissociated cells in the MCD medium and the number of separated cells in the control medium. The proportion of dissociated cells increases in correlation with the duration of the MCD treatment (0.5 h < 1 h < 4 h). Images above the columns represent the corresponding Dsc2 distribution. Thirty minute (A) and 1-h (B) incubation in MCD showed a continuous Dsc2 distribution, whereas after 4-h incubation (C, arrows) in MCD, a discontinuous Dsc2 distribution was found at places at which the cells had become disconnected. The strength of cell-cell junctions was restored when MCD loaded with cholesterol (MCD-CHOL) was applied to cells for 1 h (D). Error bars represent the SEM from an experiment in which each condition was tested three times in triplicate.

Fig. 6. Effect of MCD on membrane distribution of Dsc2 and Oly. A, cells were grown in control and MCD media and labeled with Oly. In the control treatment, Dsc2 overlapped with Oly (arrows, upper panel). Oly labeling completely disappeared from the plasma membrane after cholesterol depletion (lower panel) but the Dsc2 distribution did not disappear. Scale bar, 10 μm . B, depletion of membrane cholesterol with MCD released Dsc2 from DRMs and non-DRMs (MCD). Dsc2 distribution in DRMs was returned when MCD-cholesterol was applied to cells (MCD-CHOL). Treatment with cholesterol oxidase (CO) completely released Dsc2 from DRMs. C, effect of MCD on membrane distribution of Dsg2. Fraction 5 and DRM fractions 6 and 7 were pooled from sucrose gradients after centrifugation of Triton X-100 lysed cells. Dsg2 is released from fraction 5 and from DRM fractions 6 and 7 in comparison to control fractions.

FIGURES

Figure 1

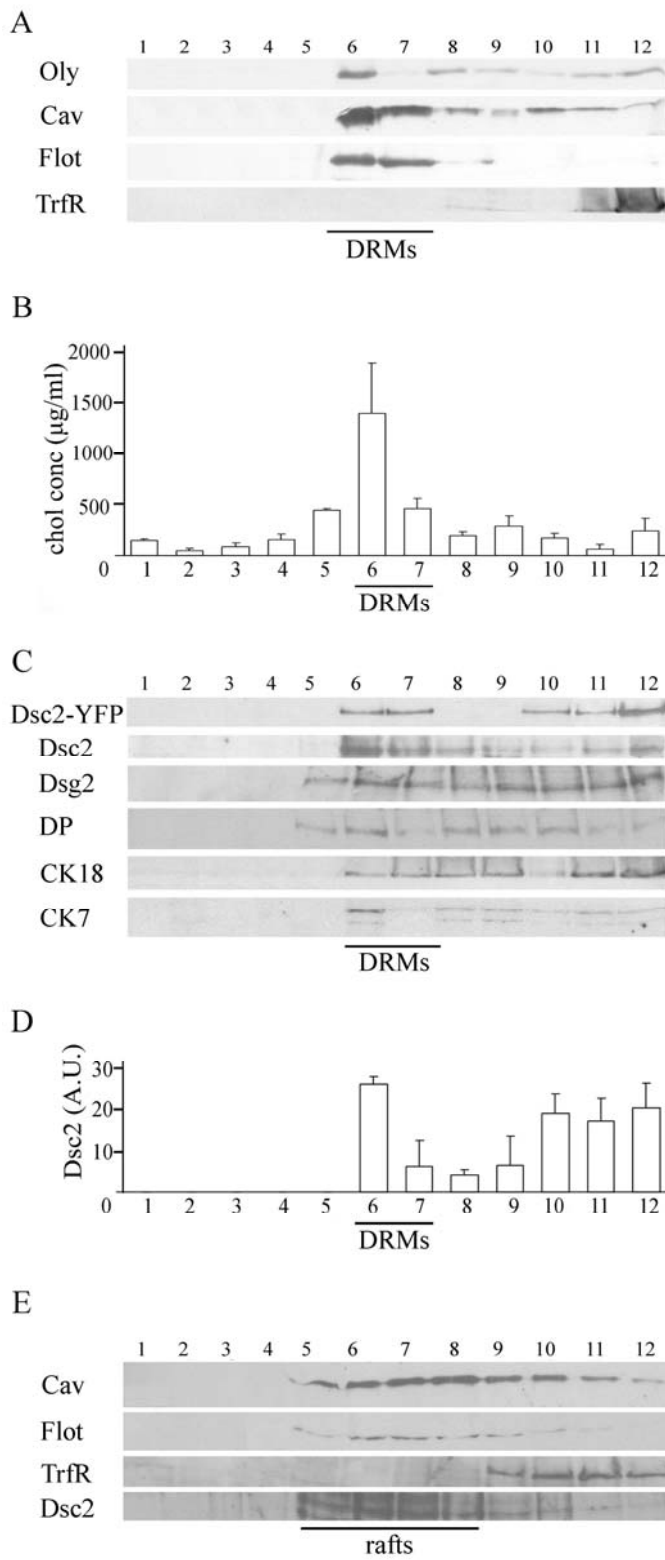


Figure 2

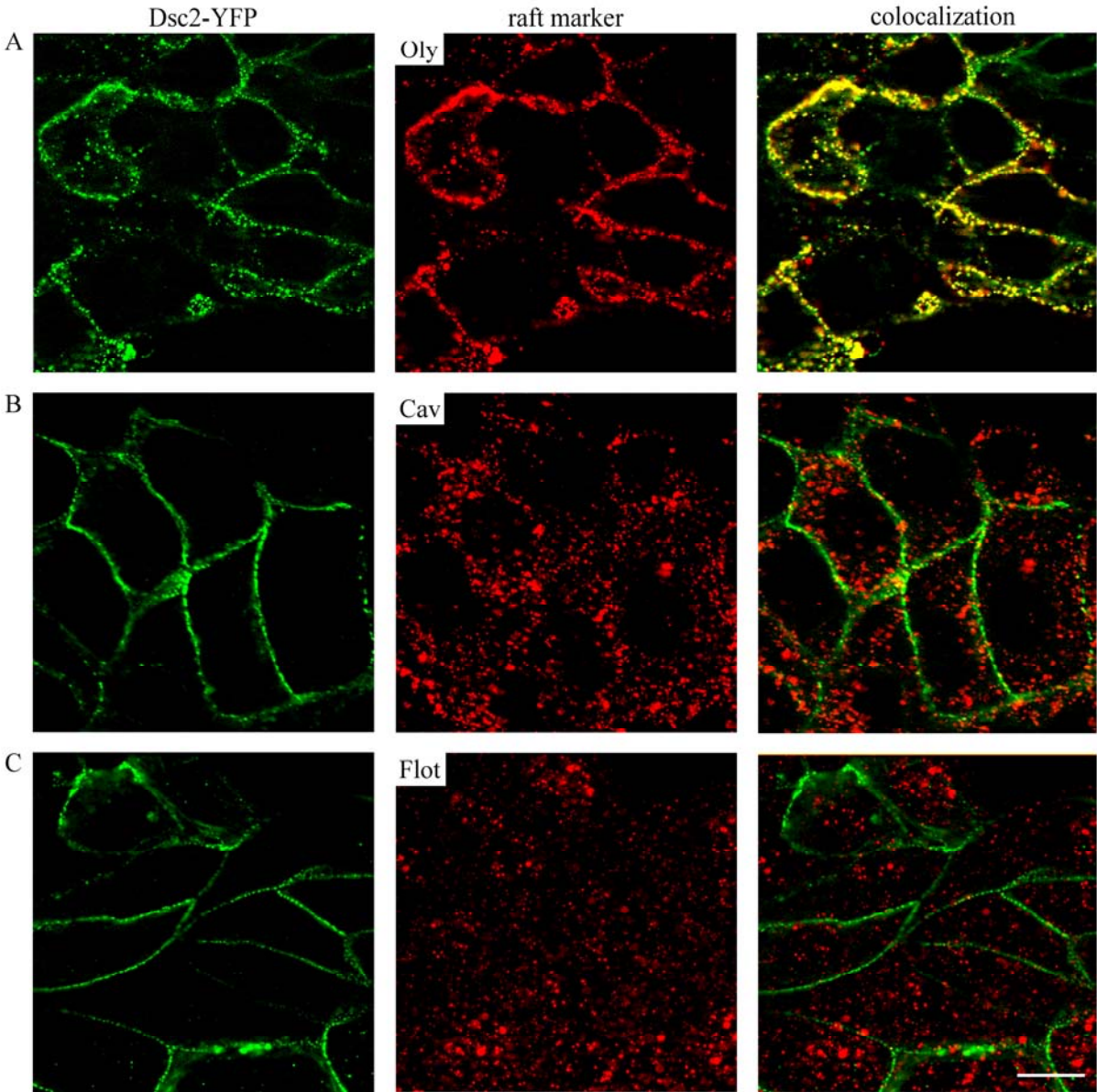


Figure 3

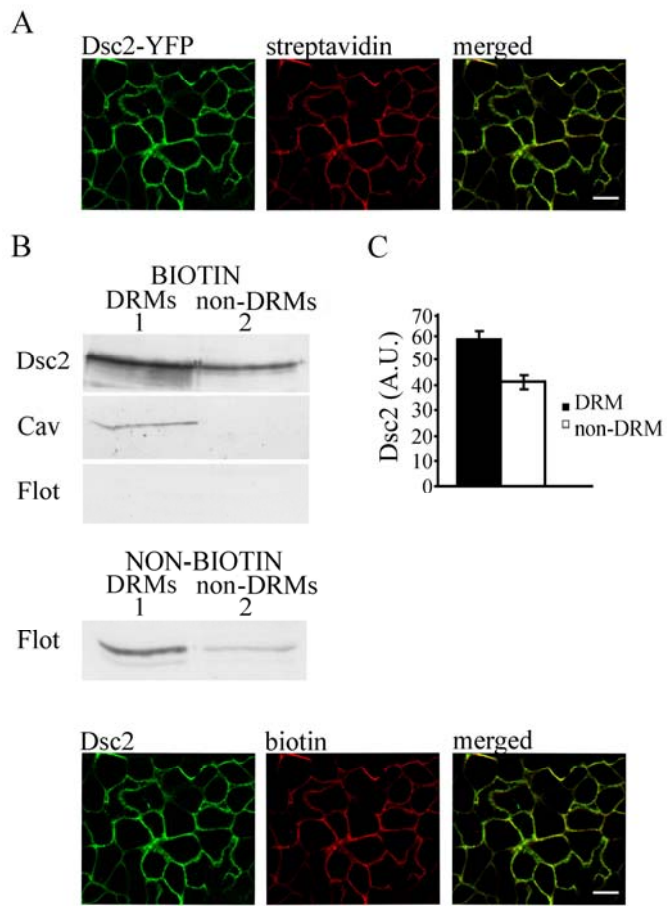


Figure 4

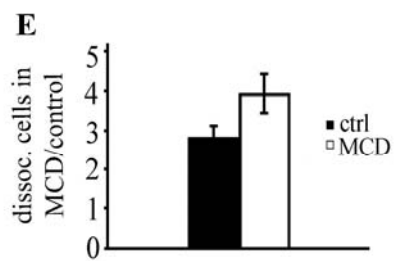
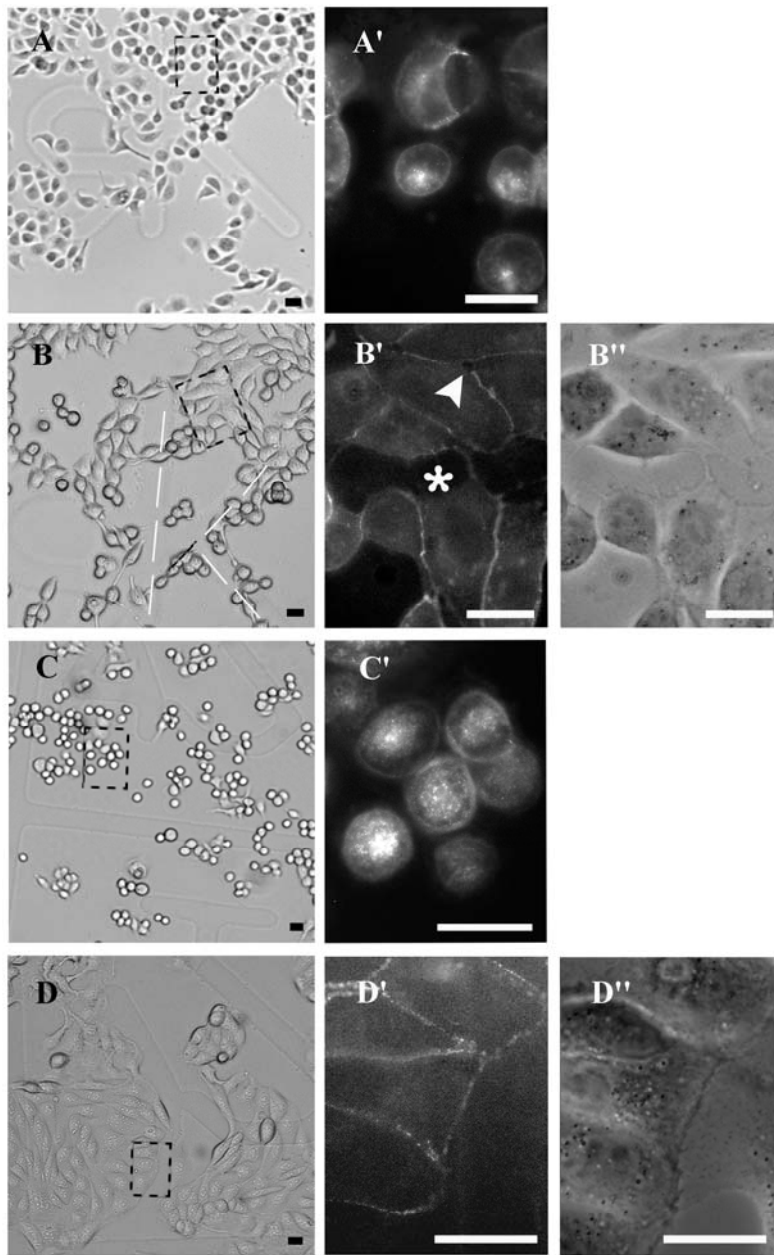


Figure 5

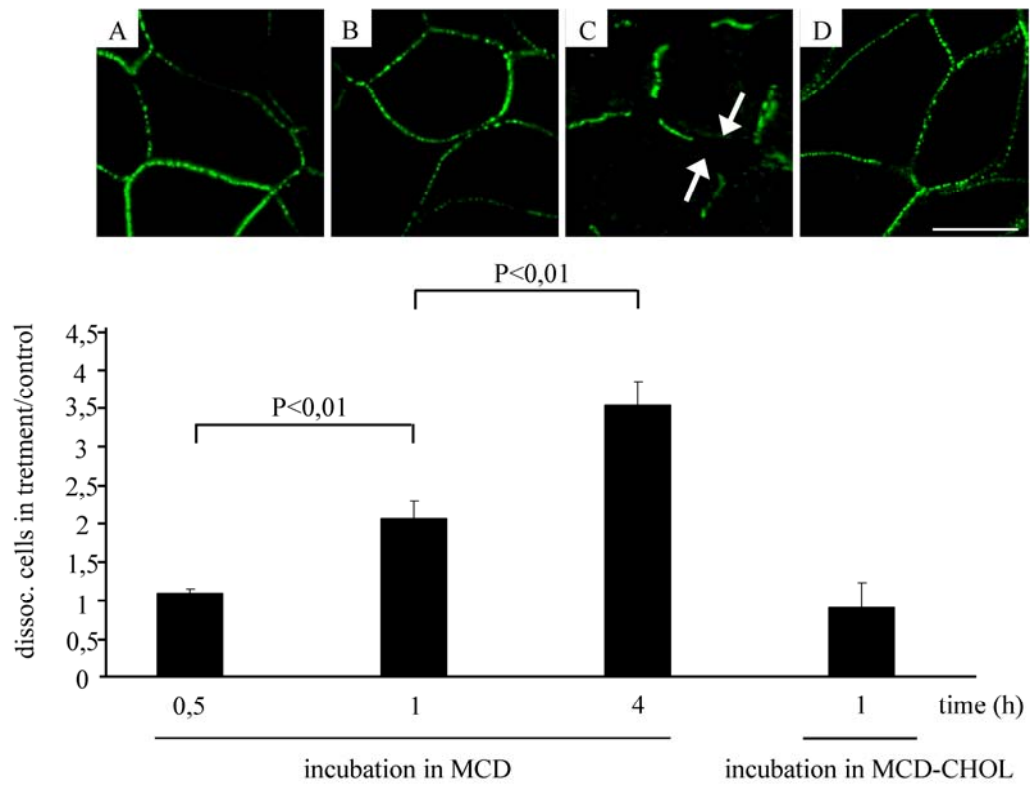


Figure 6

